

## Article

# Probability Model of Riding Behavior Choice of Two-Wheelers under the Influence of the Subsidence Area of a Manhole Cover

Dan Zhou \*, Qingwei Hu, Xin Sun, Weizhen Yao, Guobin Gu, Ruixin Yang and Congruo Ma

School of Architecture and Transportation Engineering, Guilin University of Electronic Technology, Jinji Road 1#, Guilin 541004, China; 19152301006@mails.guet.edu.cn (Q.H.); sunx\_lynn@163.com (X.S.); yaoweizhen1007@163.com (W.Y.); 20152202006@mails.guet.edu.cn (G.G.); cj541@sina.com (R.Y.); mcr\_1996@163.com (C.M.)

\* Correspondence: zhoudan\_5460@126.com; Tel.: +86-0773-230-3726

**Abstract:** To objectively evaluate the influence of the subsidence area of a manhole cover on the riding behavior of two-wheeler riders in urban bicycle lanes, a probability model of riding behavior of two-wheeler riders was established. The main factors influencing the probability of riding behaviors under the condition of the subsidence area of a manhole cover are investigated. Based on the field data of 10 survey sections in Guilin, the regression models between the selected probability of independent riding behavior, combined riding behavior and the main influencing factors are respectively established by using the multiple regression analysis method. The results show that the selected probabilities of deceleration riding behavior and original-speed riding behavior have a linear regression relationship with the subsidence depth of the manhole cover and the lane integrity. The subsidence depth of manhole covers is positively correlated with the probability of deceleration riding behavior and negatively correlated with the probability of original-speed riding behavior; lane integrity is positively correlated with both the probability of deceleration riding behavior and the probability of original-speed riding behavior. The data goodness-of-fit value for the relevant influence factors in the two models is 0.941 and 0.900, respectively. The probability of acceleration riding behavior has a linear regression relationship with the lane integrity and section flow. Lane integrity is negatively correlated with the probability of acceleration riding behavior and positively correlated with section flow. The data goodness-of-fit value for the relevant influence factors is 0.821. The probabilities of straight riding behavior and detour riding behavior have a linear regression relationship with the subsidence depth of manhole covers and the minor width of the flat part. The subsidence depth of a manhole cover is negatively correlated with the probability of straight riding behavior and positively correlated with the probability of detour riding behavior. The minor width of flat part is negatively correlated with the probability of straight riding behavior and positively correlated with the probability of detour riding behavior. The data goodness-of-fit value for the relevant influence factors in the two models is 0.601 and 0.603, respectively. The results provide the theoretical basis for the evaluation of the severity and optimization design of the subsidence of manhole covers in urban bicycle lanes.

**Keywords:** traffic safety; multiple regression; the subsidence of manhole covers; two-wheeler; probability of riding behavior



**Citation:** Zhou, D.; Hu, Q.; Sun, X.; Yao, W.; Gu, G.; Yang, R.; Ma, C. Probability Model of Riding Behavior Choice of Two-Wheelers under the Influence of the Subsidence Area of a Manhole Cover. *Sustainability* **2022**, *14*, 3532. <https://doi.org/10.3390/su14063532>

Academic Editors: Efthimios Bothos, Panagiotis Georgakis, Babis Magoutas and Michiel de Bok

Received: 29 January 2022

Accepted: 14 March 2022

Published: 17 March 2022

**Publisher's Note:** MDPI stays neutral with regard to jurisdictional claims in published maps and institutional affiliations.



**Copyright:** © 2022 by the authors. Licensee MDPI, Basel, Switzerland. This article is an open access article distributed under the terms and conditions of the Creative Commons Attribution (CC BY) license (<https://creativecommons.org/licenses/by/4.0/>).

## 1. Introduction

In recent years, due to the negative effects of traffic congestion, air pollution and traffic accidents, many major cities in China have enacted ordinances banning fuel-fueled motorcycles from urban roads [1,2]. As a result, two-wheeled motorcycles are gradually being replaced by electric two-wheelers and bicycles in many major cities in China. Two types of two-wheelers studied in this paper include electric two-wheelers and human-powered bicycles. The two-wheelers studied in this paper are more energy efficient and

low carbon than fuel-powered motor vehicles, which can help protect the environment to a great extent [3]. They are also a fast way to connect with buses and subways, which can improve the service radius of public transportation stations [4]. Electric two-wheelers and human-powered bicycles will be more widely used as low-carbon and environmentally friendly transportation options [3].

During the road expansion and laying of underground pipelines, many inspection wells are distributed in urban bicycle lanes. Due to long-term rolling or subsidence, the manhole cover of these inspection wells has different degrees of subsidence. Many scholars have carried out relevant research on the damage mechanism of manhole covers. Zhao et al. [5] established the vehicle–manhole cover coupling vibration model based on the investigation. The study established the structural model of the inspection well and the pavement around the inspection well. The results showed that the damage radius of the pavement around the manhole cover is generally within 1.2 m, and the flatness of the pavement around the manhole cover is much worse than that of the conventional pavement. Yu et al. [6] found that the damages to the manhole cover are mainly the cracking of the pavement around the manhole cover and the inclined depression of the manhole cover through the investigation of inspection wells on the main urban roads in Qingdao. The number of damaged wells is related to factors such as construction technology, construction period, load, inspection well location and manhole cover quality. For example, because two-wheelers have a lower road load, the severity of manhole cover diseases is much lower than in the motor vehicle lane. Due to the lighter weight of two-wheelers, the phenomenon of bumping is more serious when the two-wheelers pass through the subsidence area. The vibration filtering capacity of the two-wheelers' suspension systems is limited, which greatly reduces the riding comfort of riders when they pass through the subsidence area.

It is found that there is still a further demand from road users for the improvement of road driving comfort [7]; in the current study, the correlation between pavement unflatness and driving comfort has mainly focused on motor vehicles. Wang et al. [8] proposed that if the pavement damage condition is poor, the corresponding pavement flatness is also poor. From the standpoint of pavement riding comfort, different types of damage have different effects on the driving comfort of the pavement. Shan et al. [9,10] explored the relationship between pavement unflatness and driving comfort by establishing a ten-degree-of-freedom whole-vehicle model that conforms to the actual vibration of the vehicle and adjusted the pavement unflatness classification from the perspective of comfort. Lu et al. [11] conducted a simulation analysis of multi-passenger vehicle smoothness by establishing a pavement unflatness model. The results showed that the higher the pavement unflatness, the bumpier the road will be and the worse the driving comfort will be. Guan et al. [12] proposed that road flatness is an important factor affecting riding comfort, and unfalt pavement enhances the body vibration of the driving vehicle and reduces the driving quality of the vehicle. Some scholars have also suggested that road surface flatness is important for the riding comfort of two-wheelers. Zhao et al. [13] proposed that bicycle lane pavement flatness is a necessary requirement in the construction standards of bicycle-friendly cities based on the Kano model. Xiao et al. [14] proposed that when there are bicycle lanes throughout the route and the road itself are relatively smooth, it can give a better riding experience.

The research on driving behavior under damaged road conditions mainly focuses on motor vehicle driving behavior. Among them, Chen et al. [15] discussed parameters of motor vehicle traffic flow under different damaged pavement grade conditions and analyzed the influence of pavement damage on saturated headway and average speed. The recommended value of capacity in urban road sections under different pavement damage levels was presented. Chen et al. [16] studied the lane-changing characteristics of motor vehicles with different types of drivers under the condition of pavement damage by using cellular automata theory.

The research on two-wheeler riding behavior mainly focuses on the overtaking behaviors of bicycles. Khan et al. [17] studied the overtaking process in bicycle lanes. Chen et al. [18] studied the impact of overtaking interference on bicycles. According to

probability theory, widening the width of bicycle lane and setting speed limit conditions can effectively reduce the interference of overtaking behavior on other two-wheelers traveling in the same direction. Xu et al. [19] proposed an overtaking event number model based on mixed bicycle flow and discovered a relationship between key influencing factors and the number of overtaking events. Li et al. [20] classified overtaking events as free overtaking, adjacent overtaking and blocked overtaking according to the adjacent distance of riders. Based on that, the calculation model for overtaking events was established.

In addition to the study of overtaking, many Chinese scholars have carried out research on the riding behavior of two-wheelers under the interference conditions of different traffic environments. Dong et al. [21] built a bicycle simulation model including the main behavior characteristics of bicycle overtaking and emergency avoidance under the condition of mixed traffic flow interference at intersections. Kuang et al. [22] proposed a cellular automata model of non-motor vehicle flow based on a mixed retrograde and non-motor vehicle traffic environment and explored the relationship between the proportion of retrograde vehicles and lane change probability. Ping et al. [23] established a basic capacity model of non-motor vehicles based on the condition of interference of passengers entering and leaving the bus station. The research showed that the conflict between passengers entering and leaving the bus station and non-motor vehicles has a great impact on the capacity of the bicycle lane. Wen et al. [24] studied the micro behavioral characteristics between two-wheelers and pedestrians in a shared street environment and proposed the conflict probability under different flow conditions. Ye et al. [25,26] explored the impact of on-road parking set in a physically isolated bicycle lane on non-motor vehicle traffic operations. The travel time, speed model and capacity model of non-motor vehicles were respectively constructed.

The above research on two-wheelers is mainly based on the macro and micro riding behaviors in the interference environment of motor vehicles, non-motor vehicles and pedestrians. There are few studies on the interference of the pavement environment, especially the pavement damage environment, on the operation of two-wheelers. The research on riding behavior under pavement damage mainly focuses on motor vehicles. Due to the characteristics of two-wheelers, pavement damage has a great impact on the riding comfort of two-wheelers. There are great differences in riding psychological and physiological characteristics between two-wheeler riders and motor vehicle riders [27]. There are also great differences in running tracks and speed characteristics between two-wheeler riders and motor vehicle riders [28]. When non-motor vehicles perform emergency operations such as deceleration or avoidance, it is easier to produce various traffic safety problems than motor vehicles.

The subsidence of a manhole cover is the most common cause of pavement damage in urban bicycle lanes. This study investigates the effects of size and depth characteristics, location characteristics and different traffic characteristics of the different subsidence of manhole covers in bicycle lanes on the selection of riding behavior of two-wheelers. This study puts forward the definition of two-wheeler riding behavior under the condition of the subsidence of manhole covers in urban bicycle lanes. The study explores the main categories of factors that influence riding behavior selection. The study analyzes the influence of various influencing factors on the probabilities of two-wheeler riding behaviors by using multiple regression analysis. A probability model for the selection of two-wheeler riding behavior under the condition of manhole cover subsidence is developed. This paper provides recommendations and methods for city and traffic management based on the fitted theoretical model. This study can provide theoretical support for the study of subsidence repair treatment of manhole covers and two-wheeler operation safety in independent bicycle lanes.

## 2. Data Source

### 2.1. Survey Section

Guilin is famous as a scenic tourist city and a historical and cultural city in China. There are beautiful hills with karst geomorphic features in the city. Many of the top tourist

attractions in Guilin are concentrated in the main urban areas of the city, which attracts large numbers of tourists from all over the world every year. The urban economic growth point is mainly driven by tourism. Guilin has a small urban area with six major districts. The city's terrain is flat and has an independent non-motor vehicle road network distributed in the six major districts. The per capita non-motor vehicle ownership in Guilin ranks among the top in China. The commuter modes of Guilin urban residents are mainly non-motor vehicle transportation and public bus transportation. This study mainly selects the urban bicycle lane with isolation facilities between the bicycle lane and the motor vehicle lane in the urban area of Guilin as the research object. The selection principles of road sections for the field investigation include the following: (1) The investigated road needs to have an independent bicycle lane with continuous isolation facilities between the bicycle lane and the motor vehicle lane. The lane width is required to be greater than 2 m. (2) The road sections are straight with good visibility. There are no blind spots, and no road transition sections in these sections. (3) The sections must be at least 30 m apart from the upstream and the downstream intersections, respectively. There are no bus stops or roadside parking facilities in these sections. (4) There is only one subsidence area of a manhole cover in an investigated section. The pavement within 20 m upstream and 10 m downstream of the section is in good condition. (5) The subsidence area of the manhole cover is easy to recognize. (6) Good weather conditions are to be considered. The survey time should be 7:00 a.m.–9:00 a.m., 11:00 a.m.–1:00 p.m., and 4:00 p.m.–6:00 p.m. on working days. The traffic load coefficient during the survey period was less than 0.7. In this study, 10 main road sections were selected for field investigation. The basic information for each section is shown in Table 1. The actual scene of the main types of subsidence areas is shown in Figure 1. The actual scene of each survey section is shown in Figure 2.

**Table 1.** Basic information of the survey sections.

| Number | Survey Section              | Isolation Facilities | Width of Lane/m | Subsidence Depth/cm | Width of Subsidence/m |
|--------|-----------------------------|----------------------|-----------------|---------------------|-----------------------|
| 1      | Fangxiang Road              | Greenbelt            | 3.0             | 1.5                 | 0.77                  |
| 2      | Zhongshan Middle Road       | Greenbelt            | 3.5             | 0.8                 | 0.70                  |
| 3      | Cuizhu Road section A       | Greenbelt            | 3.5             | 2.0                 | 0.72                  |
| 4      | Jiefang East Road section A | Greenbelt            | 3.5             | 2.1                 | 0.71                  |
| 5      | Jiefang East Road section B | Greenbelt            | 3.5             | 2.3                 | 0.73                  |
| 6      | Liuhe Road                  | Greenbelt            | 4.0             | 1.3                 | 0.72                  |
| 7      | Cuizhu Road section B       | Greenbelt            | 4.5             | 1.8                 | 0.72                  |
| 8      | Zhongshan North Road        | Fence                | 4.5             | 2.1                 | 0.72                  |
| 9      | Jiefang East Road section C | Greenbelt            | 4.5             | 3.2                 | 0.86                  |
| 10     | North Ring 2nd Road         | Greenbelt            | 5.0             | 1.7                 | 0.96                  |

## 2.2. Data Collection and Processing

### 2.2.1. Depth Measurement of the Subsidence Area

In this paper, the subsidence depth of 10 manhole covers in all investigated sections was measured with steel tape. The field measurement diagram is shown in Figure 3. Two line segments, AB and CD, were created, one parallel to the riding direction and the other perpendicular to the riding direction. The line segments AB and CD intersect at the center of figure O of the subsidence area. Firstly, a steel tape was placed horizontally on the line segment AB. To measure the depths at the three points successively, another steel tape was placed in the direction perpendicular to the road at the point O and the midpoints (points E and F) of line segment OA, OB. Secondly, the first steel tape was placed horizontally on the line segment CD. The second steel tape was placed in the direction perpendicular to the road at the point O and the midpoints (points G and H) of line segment OC, OD to measure the depths at the three points successively. Finally, the average value of all the depths was regarded as the subsidence depth of the manhole cover.

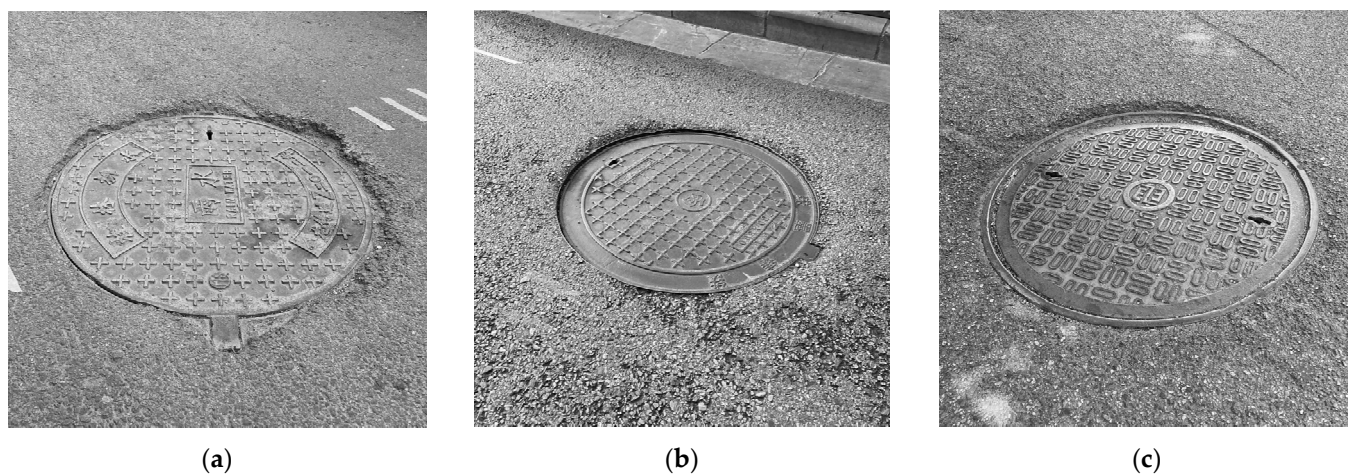


Figure 1. The actual scene of a subsidence area: (a) Fangxiang Road, (b) Jiefang East Road section A, and (c) Jiefang East Road section C.



(a)



(b)



(c)



(d)



(e)



(f)

Figure 2. Cont.

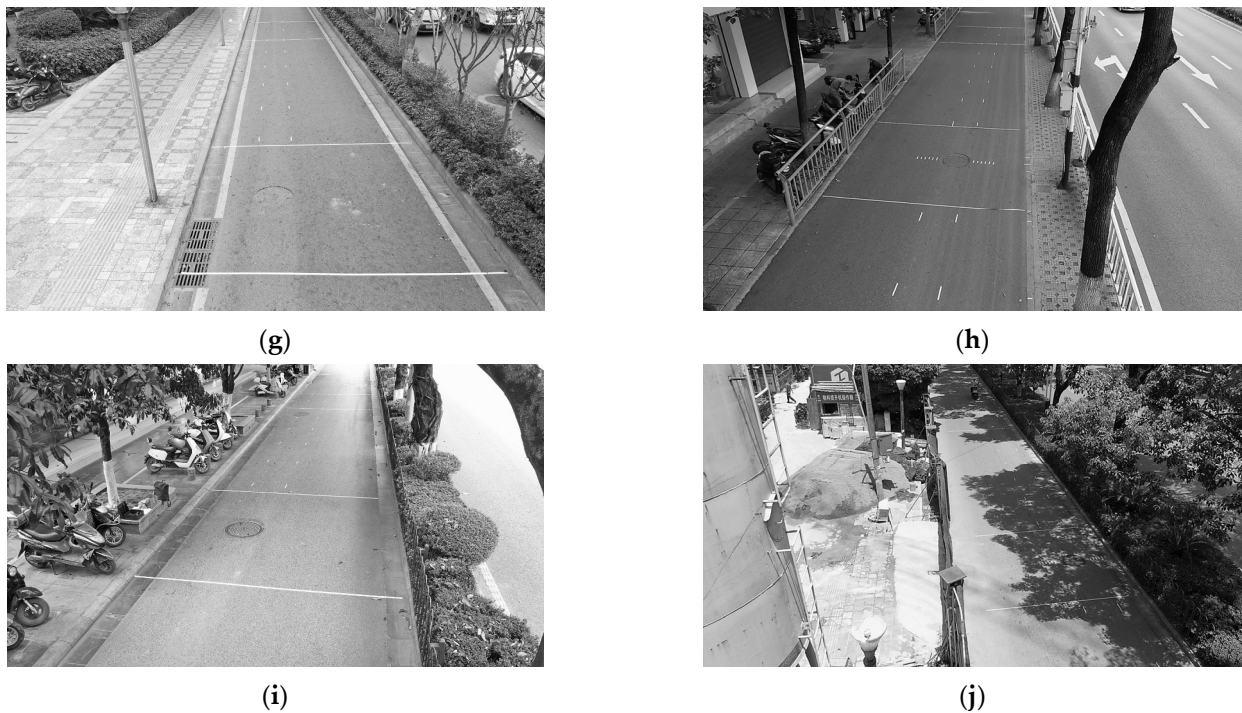


**Figure 2.** The actual scene of each subsidence area of the survey sections. (a) Fangxiang Road, (b) Zhongshan Middle Road, (c) Cuizhu Road section A, (d) Jiefang East Road section A, (e) Jiefang East Road section B, (f) Liuhe Road, (g) Cuizhu Road section B, (h) Zhongshan North Road, (i) Jiefang East Road section C, and (j) North Ring 2nd Road.

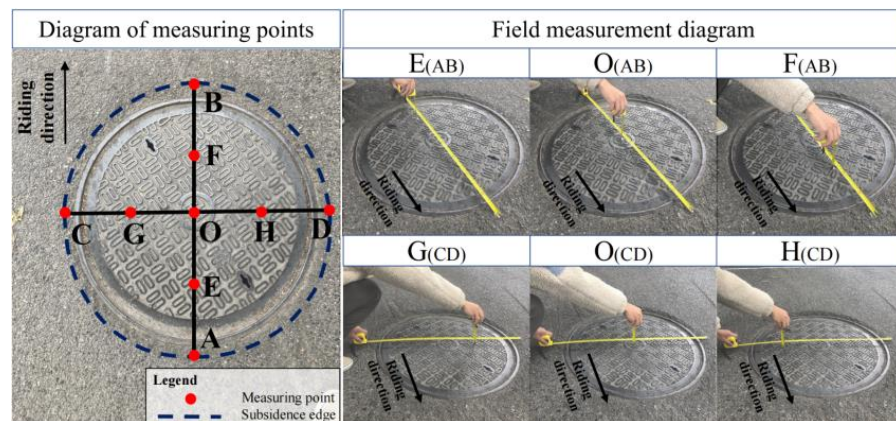


**Figure 3.** Measurement of settlement depth of the manhole cover and its surrounding.

### 2.2.2. Definition of Upstream Virtual Traffic Zone in the Survey Area

This study used the video survey method to collect the field data. As shown in Figure 3, two parallel lines were made perpendicular to the CD line segment, passing through point C and point D. The area along the upstream of the manhole cover between the parallel lines is the upstream virtual traffic zone. A group of short marking lines were drawn along the riding direction every 2 m on both sides of the upstream virtual traffic zone (as shown in Figure 4).

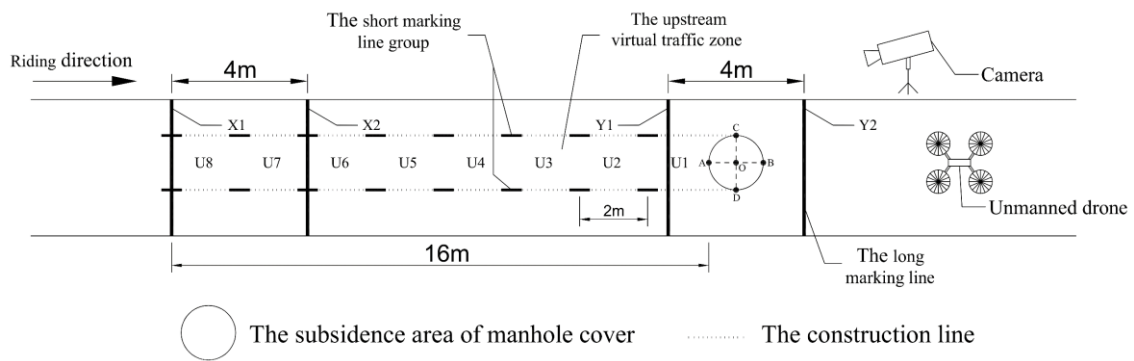


Figure 4. Layout of survey site.

The area between two adjacent short marking line groups along the riding direction is defined as a longitudinal sub-interval, which is numbered as  $U_{\delta}$ , ( $\delta = 1, 2, 3, \dots, n$ ) successively from the subsidence area to the direction away from the area. Overall, 1103 valid samples were selected from 1326 samples and counted. The number of two-wheelers riding out of the upstream virtual traffic zone from each longitudinal distance interval from the subsidence area is shown in Figure 5. The abscissa is each longitudinal distance interval, and the ordinate is the number of two-wheelers riding out of the upstream virtual traffic lane. When the two-wheelers leave the upstream virtual traffic zone, the longitudinal distance from the subsidence area is concentrated at 0–14 m. Therefore, the length of the upstream virtual traffic zone was set at 16 m in this study. The zone was divided into eight groups of longitudinal distance segments. The layout of the upstream virtual traffic zone of the survey section is shown in Figure 5.

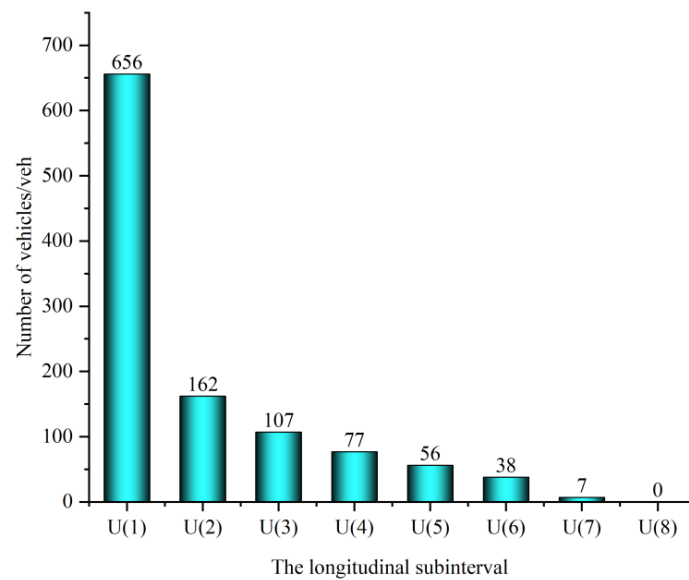


Figure 5. Frequency of two-wheelers leaving each interval.

### 2.2.3. Definition of Velocity Collection Area

Two groups of long marking lines with an interval of 4 m each were drawn perpendicular to the riding direction on the pavement of the bicycle lane. Each group includes two long marking lines, which are represented by group X and group Y, respectively. The two long marking lines of group X were respectively drawn 16 m and 12 m away from the manhole cover upstream of the subsidence area. They are called long marking line X1 and long marking line X2. Based on the line segment CD of the subsidence area (as shown in Figure 3), the long marking line Y1 in group Y was drawn at a position 2 m away from the manhole cover in the upstream of the subsidence area. The long marking line Y2 in group

Y was drawn at the position 2 m away from the manhole cover downstream of subsidence area. The total length of the survey section is  $(18 + L_m/2)$  m, where  $L_m$  is the length of line segment AB shown in Figure 3. The field survey layout of the velocity collection area is shown in Figure 5.

#### 2.2.4. Collection Requirements

Unmanned aerial vehicles and cameras were used to capture video and obtain traffic flow data. The research object of this study was two-wheelers passing through the upstream virtual traffic zone in the survey sections. The traffic video was decomposed into continuous pictures frame by frame by using video software for analysis [29]. The video data extracted from this study include the following: (1) Record the time when the front wheel of each two-wheeler rolls over the four long marking lines X1, X2, Y1 and Y2 successively with a recording accuracy of 0.04 s. (2) Determine the rider's gender and age range from multiple perspectives based on the rider's facial features, hair features, clothing style, accessory features and height features. (3) Track whether the rider exits the upstream virtual traffic zone. If he drives out of the upstream virtual traffic zone, note the corresponding longitudinal section number. (4) Record whether two-wheelers pass through the subsidence area of the manhole cover. If they do not pass through the subsidence area, record the relative position between the two-wheelers and the subsidence area at the time when they pass through the area from either side of the subsidence area. (5) Count the number of two-wheelers that roll down the long marking line X1, using 10 s as the statistical interval. The real-time data such as gender, age range, speed in each range, whether to drive out of the upstream virtual traffic zone and the situation of riding out of the range can be collected through video analysis. These data provide samples for subsequent model establishment.

#### 2.2.5. Data Statistics and Pre-Processing

In this paper, we define the interval speed between X1 and X2 as the initial speed, the interval speed between Y1 and Y2 as the end speed and the difference between the initial speed and the end speed as the difference in speed change. The data of initial speed, difference in speed change and riding away from the longitudinal subinterval for all samples are statistically analyzed, scatter plots are drawn and fluctuation range boundary functions are found.

Firstly, the relationship between the initial speed and the difference in speed change for the full sample is investigated, and the relevant scatter plot is shown in Figure 6.

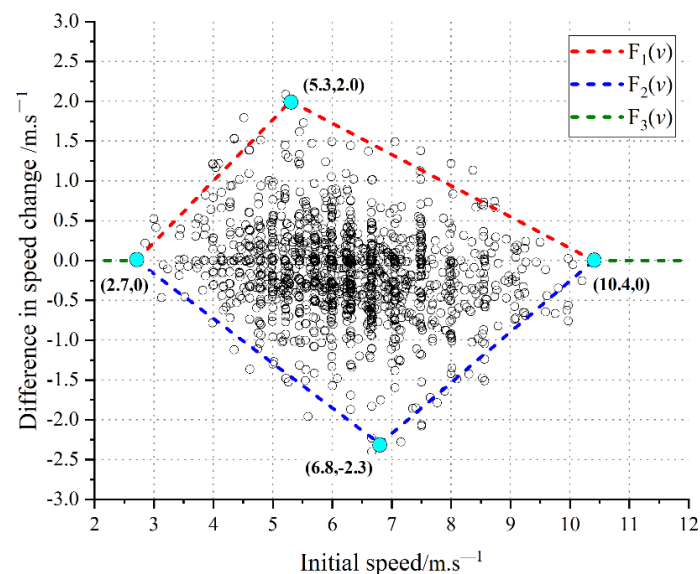


**Figure 6.** Relationship between initial speed and difference in speed change.

In the acceleration riding behavior, when the initial speed reaches 5.3 m/s, the speed fluctuation range of the two-wheeler reaches a maximum of 2.0 m/s. In the deceleration riding behavior, when the initial speed reaches 6.8 m/s, the speed fluctuation range of the two-wheeler reaches a maximum of  $-2.3$  m/s. When the initial speed is less than 2.7 m/s or the initial speed is greater than 10.4 m/s, the speed fluctuation range of the two-wheeler is approximately 0.

$$F_1(v) = \begin{cases} 0.769v - 2.0763, v \in (2.7, 5.3) \\ -0.392v + 4.0768, v \in [5.3, 10.4) \end{cases} \quad (1)$$

$$F_2(v) = \begin{cases} -0.561v + 1.5147, v \in (2.7, 6.8) \\ 0.639v - 6.6456, v \in [6.8, 10.4) \end{cases} \quad (2)$$

$$F_3(v) = 0, v \in (0, 2.7] \cup [10.4, +\infty) \quad (3)$$

where  $v$  is the initial speed in m/s,  $F_1(v)$  is the upper limit of fluctuation in m/s,  $F_2(v)$  is the lower limit of fluctuation in m/s and  $F_3(v)$  is the limit of no fluctuation m/s.

The relationship between the initial speed and its behavior in selecting longitudinal subintervals to leave the upstream virtual traffic zone is explored. The scatter plot of the initial speed statistics of the two-wheelers leaving each longitudinal subinterval is shown in Figure 7.

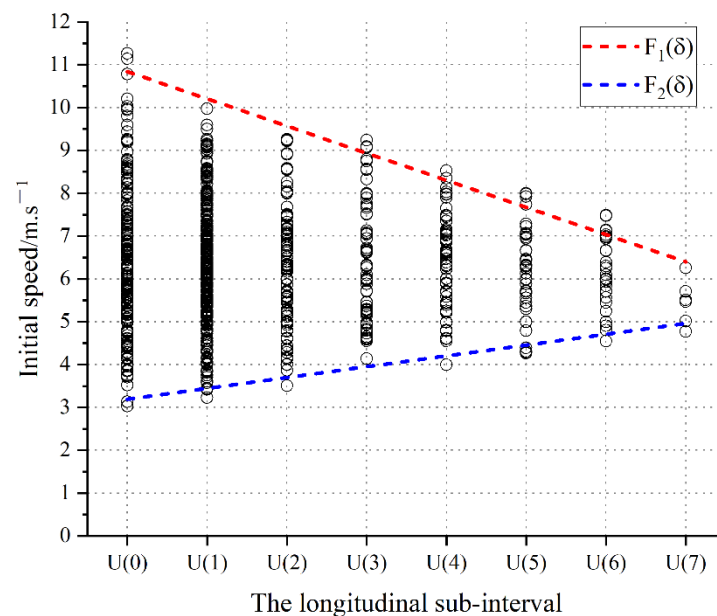


**Figure 7.** Statistical relationship between a longitudinal subinterval number and the initial speed of a two-wheeler leaving from that longitudinal subinterval.

In Figure 7,  $U(0)$  indicates that the two-wheeler does not leave the upstream virtual traffic zone and roll over the subsidence area. The horizontal coordinates of the scatter points in the figure indicate the number of the longitudinal subinterval from which the two-wheeler is selected to leave the upstream virtual traffic zone, and the vertical coordinates of the scatter points indicate the initial speed of the two-wheeler selected to leave from that longitudinal subinterval. From the Figure 7, it can be seen that the further the longitudinal subinterval is from the subsidence area, the smaller the distribution of speed values for all two-wheelers leaving the upstream virtual traffic zone from that longitudinal subinterval.

Expressing the above characteristics as a function of the upper and lower limits of the velocity distribution, the function is shown in Equation (4).

$$\begin{cases} F_1(\delta) = -0.634\delta + 10.838, \delta = 0, 1, \dots, 6, 7 \\ F_2(\delta) = 0.253\delta + 3.192, \delta = 0, 1, \dots, 6, 7 \end{cases} \quad (4)$$

where  $F_1(\delta)$  is the upper limit of the initial speed distribution of all two-wheelers leaving different longitudinal subintervals in m/s and  $F_2(\delta)$  is the lower limit of the initial speed distribution of all two-wheelers leaving different longitudinal subintervals in m/s.

### 3. Methodology

#### 3.1. Classification and Definition of Riding Behavior

The behavioral strategies of two-wheeler riders facing the subsidence area of a manhole cover can be divided into two categories. One is a speed behavioral strategy, and the other is a trajectory behavioral strategy. Speed riding behavior includes three riding behaviors: deceleration riding behavior, original-speed riding behavior and acceleration riding behavior. The trajectory riding behavior includes straight riding behavior and detour riding behavior.

According to the traffic survey, most riders do not use the braking device to slow down when they encounter the subsidence area of the manhole cover under non-crowded conditions. Instead, they use the sliding deceleration mode, that is, they use the friction resistance between the wheels and the road to slow down. In this process, the speed change of two-wheelers is relatively gentle. During the process of continuing to run at the original speed or accelerating, the two-wheelers' speed shows a slowly changing as well. Based on this, the study defines the riding behavior in which the two-wheelers' deceleration value is greater than 5% of the two-wheelers' initial speed or the absolute deceleration value is more than 1 km/h, which is called deceleration riding behavior. When the two-wheelers' acceleration value is greater than 5% of the two-wheelers' initial speed or the absolute acceleration value exceeds 1 km/h, the riding behavior is called acceleration riding behavior. When the absolute speed change rate of the two-wheelers is less than 5% of the initial speed or the absolute speed change value is less than 1 km/h, the riding behavior is called original-speed riding behavior.

Trajectory riding behavior includes straight riding behavior and detour riding behavior. Straight riding behavior is a riding behavior that goes along the upstream virtual traffic zone from discovering and judging the subsidence area of a manhole cover to passing through the area. Detour riding behavior is the riding behavior that drives away from the upstream virtual traffic zone to discover and judge the subsidence area of a manhole cover to allow for passing from either side of the area. Two types of trajectory riding behavior are shown in Figure 8. Figure 9 shows the actual scene of nodes in each stage of the rider's behavior execution in the survey section. In Figure 9, "a" shows the entering area, "b" shows the area of performing the detour, "c" shows the riders passing the subsidence area and "d" shows the exiting area. The identification–decision stage is from "a" to "b", the executive stage is from "b" to "c" and the returning to normal riding stage is from "d".

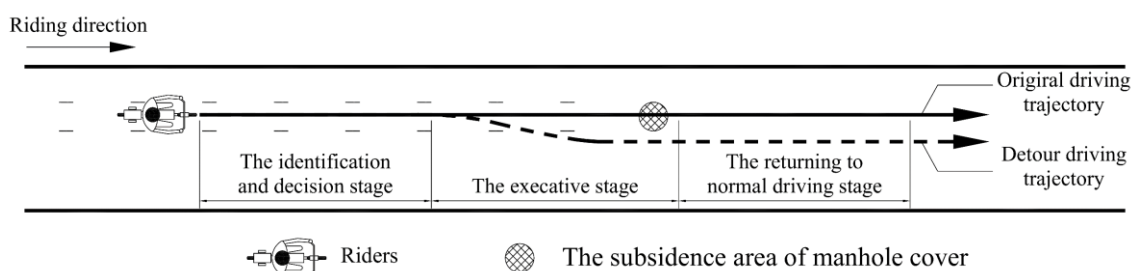


Figure 8. Schematic diagram of trajectory riding behavior.

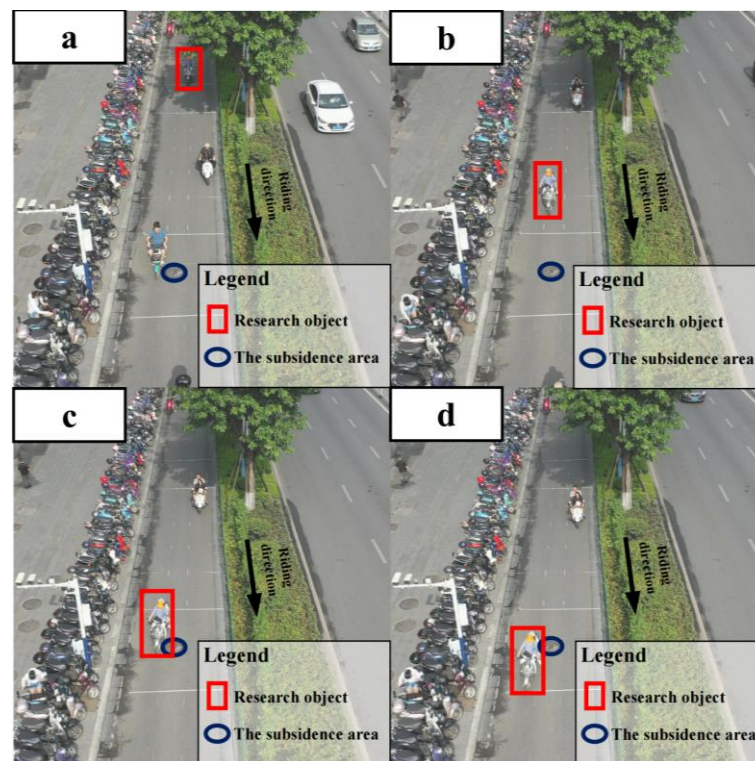


Figure 9. The actual scene of trajectory riding behavior of nodes in each stage.

Six kinds of combined riding behaviors can be obtained by combining any riding behavior in speed riding behaviors with any riding behavior in trajectory riding behaviors. The six kinds include deceleration, straight riding behavior, deceleration detour riding behavior, original-speed straight riding behavior, original-speed detour riding behavior, acceleration straight riding behavior and acceleration detour riding behavior. Riding behavior’s classification is shown in Table 2.

Table 2. Riding behaviors’ classification.

| Behavior Category           | Behavior Subclass  |  |
|-----------------------------|--|--|
| Independent riding behavior | Speed riding behavior  | Deceleration riding behavior<br>Original-speed riding behavior<br>Acceleration riding behavior |
|                             | Trajectory riding behavior   | Straight riding behavior<br>Detour riding behavior   |
| Combined riding behavior    | Deceleration straight riding behavior<br>Deceleration detour riding behavior<br>Original-speed straight riding behavior<br>Original-speed detour riding behavior<br>Acceleration straight riding behavior<br>Acceleration detour riding behavior |  |

### 3.2. Selected Probability of Riding Behaviors and the Influencing Factors

In this study, each riding behavior is regarded as an independent probability event.  $M$  represents all the two-wheelers passing through the upstream virtual zone.  $S_1$  is the decelerating two-wheelers.  $S_2$  is the two-wheelers that keep their original speed.  $S_3$  is the accelerating two-wheelers.  $T_1$  is the two-wheelers that choose straight riding behavior.  $T_2$

is the two-wheelers that choose detour riding behavior.  $P(x)$  is the probability of  $x$  event. Each set probability meets the following conditions:

$$P(M) = \begin{cases} P(S_1) + P(S_2) + P(S_3) = 1 \\ P(T_1) + P(T_2) = 1 \\ P(S_1T_1) + P(S_1T_2) + P(S_2T_1) + P(S_2T_2) + P(S_3T_1) + P(S_3T_2) = 1 \end{cases} \quad (5)$$

This study analyses the main factors affecting the selected probability of independent riding behaviors and the selected probability of combined riding behaviors. According to the results of existing relevant research, the driving behavior of motor vehicle drivers is mainly affected by the severity of damage, the distance between the damaged area and where it is recognized by the driver, the lane width of flat part under damaged conditions, vehicle speed and other factors. The selected probability of riding behavior is also affected by the characteristics of riders, which are mainly gender and age. This study analyses the statistical relationship between the eight influencing factors and the selected probability of riding behaviors from the perspective of traffic environment characteristics and rider characteristics. The influencing factors of riding behavior probability are shown in Table 3.

**Table 3.** Influencing factors of riding behavior probability.

| Characteristic Type                    | Influence Factor                  | Symbol     | Unit           |
|--|-----------------------------------|------------|----------------|
| Characteristics of traffic environment | Subsidence depth of manhole cover | $D$        |                |
|  | Lane integrity                    | $C_p$      | %              |
|  | Major width of flat part          | $C_{\max}$ | m              |
|  | Minor width of flat part          | $C_{\min}$ | m              |
|  | Section flow                      | $q_f$      | bike/(min · m) |
| Characteristics of riders              | Age proportion of riders          | $p_1$      | %              |
|  | Sex proportion of riders          | $p_2$      | %              |

According to the survey, the subsidence depths of manhole covers in urban bicycle lanes are mainly concentrated in a range of 0–4 cm. Two-wheelers have higher requirements for pavement flatness because two-wheelers weigh less than four-wheeled motor vehicles, and the shock absorption effect of two-wheelers' shock absorbers is poorer than that of four-wheeled motor vehicles. The subsidence depths of manhole covers in urban bicycle lanes were reclassified and primarily divided into four categories in this study, as shown in Table 4.

**Table 4.** Classification of subsidence severity and subsidence depth.

| Severity                      | Type     | Subsidence Depth/cm | Traffic Riding Experience  |
|-------------------------------|----------|---------------------|--|
| Slight subsidence             | Type I   | $0.5 \leq D < 1$    | Slight turbulence under high speed, and no obvious turbulence under medium and low speed       |
| Moderate subsidence           | Type II  | $1 \leq D < 2$      | Slight turbulence under medium and low speed, and moderate turbulence under high speed         |
| Relatively serious subsidence | Type III | $2 \leq D < 3$      | Moderate turbulence under medium and low speed, and serious turbulence under high speed        |
| Severe subsidence             | Type IV  | $3 \leq D$          | Serious turbulence under medium and low speed, dangers are prone to be caused under high speed |

To eliminate the influence of the width difference in urban bicycle lanes on the modeling, the concept of lane integrity is proposed by using the normalization method [30]. It is defined as:

$$C_p = \frac{d - w}{d} \quad (6)$$

where  $C_p$  is lane integrity,  $d$  is the width of bicycle lanes and  $w$  is the width of the subsidence area of the manhole cover. The major width of flat part is the width of wider side of the subsidence area of the manhole cover (as shown in Figure 10). The minor width of flat part is the width of narrower side of the subsidence area of the manhole cover (as shown in Figure 8). In this study, the influencing factors of riders' characteristics are age and the gender composition ratio of riders:

$$p_1 = \frac{N_y}{N_o} \quad (7)$$

$$p_2 = \frac{N_m}{N_w} \quad (8)$$

where  $p_1$  is the age composition ratio of riders,  $N_y$  is the number of young riders,  $N_o$  is the number of old riders,  $p_2$  is the gender composition ratio of riders,  $N_m$  is the number of male riders and  $N_w$  is the number of female riders.

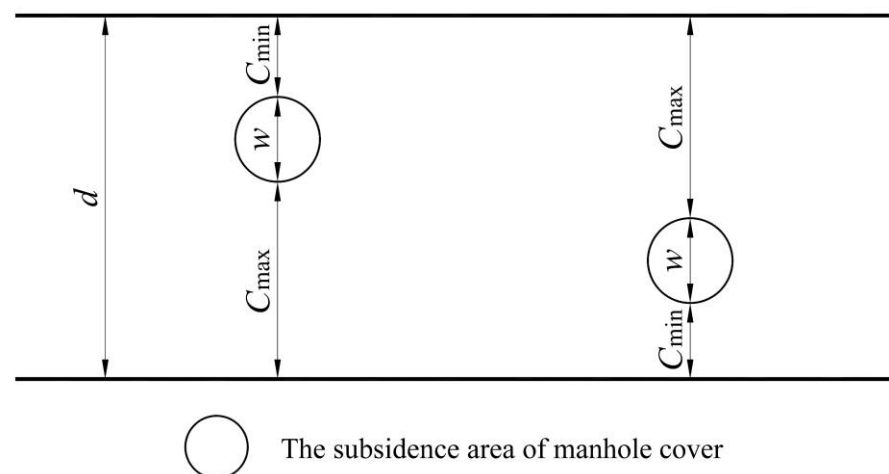


Figure 10. Width of each part in bicycle lane.

Among the influencing factors, the subsidence depths of manhole covers are set to ordered variables. That is, the type I depth of subsidence is set to "1". The type II depth of subsidence is set to "2". The type III depth of subsidence is set to "3". The type IV depth of subsidence is set to "4". Other influencing factors are set as continuous variables. Section flow and probabilities of each combined riding behavior in subsidence area are shown in Table 5.

### 3.3. Selected Probability Model of Riding Behavior

To explore the influence of each influencing factor on the selected probability of riding behavior and establish the corresponding model, the selected probability of riding behavior is modeled by multiple regression analysis. The multiple linear regression model with dependent variable  $y$  and independent variable  $\{x_1, x_2, \dots, x_k\}$  has the following general form:

$$y = \beta_0 + \beta_1 x_1 + \beta_2 x_2 + \dots + \beta_k x_k + \varepsilon \quad (9)$$

where  $\{\beta_0, \beta_1, \beta_2, \dots, \beta_k\}$  is the regression coefficient and is the  $k + 1$  parameter of the unknown coefficient. In this study, the dependent variable  $y$  is the selected probability of each riding behavior. The independent variables  $\{x_1, x_2, \dots, x_k\}$  are the corresponding influencing factors.

**Table 5.** Section flow and probabilities of each combined riding behavior.

| Location Number | $q_f$<br>Bike/(min·m) | $P(S_1T_1)$ | $P(S_1T_2)$ | $P(S_2T_1)$ | $P(S_2T_2)$ | $P(S_3T_1)$ | $P(S_3T_2)$ |
|-----------------|-----------------------|-------------|-------------|-------------|-------------|-------------|-------------|
| 1               | 3.27                  | 0.1102      | 0.1441      | 0.1186      | 0.3983      | 0.0424      | 0.1864      |
|                 | 5.27                  | 0.1009      | 0.1927      | 0.0963      | 0.3257      | 0.0642      | 0.2202      |
|                 | 8.43                  | 0.1000      | 0.2273      | 0.0727      | 0.3091      | 0.0818      | 0.2091      |
| 2               | 4.83                  | 0.0667      | 0.1250      | 0.2583      | 0.3500      | 0.1333      | 0.0667      |
|                 | 6.44                  | 0.0896      | 0.0983      | 0.2833      | 0.3109      | 0.1039      | 0.1140      |
|                 | 9.02                  | 0.0895      | 0.0903      | 0.2903      | 0.2930      | 0.1179      | 0.1190      |
| 3               | 8.10                  | 0.0973      | 0.3303      | 0.0839      | 0.2848      | 0.0464      | 0.1573      |
|                 | 11.20                 | 0.1071      | 0.3293      | 0.0864      | 0.2656      | 0.0519      | 0.1597      |
|                 | 14.07                 | 0.1260      | 0.3297      | 0.0883      | 0.2311      | 0.0622      | 0.1627      |
| 4               | 6.19                  | 0.1772      | 0.2911      | 0.0759      | 0.2785      | 0.0506      | 0.1266      |
|                 | 10.03                 | 0.1476      | 0.2667      | 0.0905      | 0.2667      | 0.0619      | 0.1619      |
|                 | 14.45                 | 0.1290      | 0.2452      | 0.0968      | 0.2903      | 0.0581      | 0.1806      |
| 5               | 9.05                  | 0.1122      | 0.3265      | 0.0510      | 0.2653      | 0.0102      | 0.2347      |
|                 | 12.23                 | 0.1528      | 0.2949      | 0.0461      | 0.2778      | 0.0092      | 0.2176      |
|                 | 15.31                 | 0.1866      | 0.2687      | 0.0373      | 0.2836      | 0.0075      | 0.2164      |
| 6               | 5.37                  | 0.0896      | 0.2769      | 0.1293      | 0.3995      | 0.0263      | 0.0814      |
|                 | 7.26                  | 0.0902      | 0.2642      | 0.1357      | 0.3979      | 0.0285      | 0.0835      |
|                 | 9.77                  | 0.0870      | 0.2740      | 0.1244      | 0.3914      | 0.0297      | 0.0935      |
| 7               | 4.35                  | 0.0988      | 0.3210      | 0.1111      | 0.4198      | 0.0000      | 0.0494      |
|                 | 5.73                  | 0.0850      | 0.3007      | 0.1307      | 0.4248      | 0.0000      | 0.0589      |
|                 | 7.42                  | 0.1053      | 0.2737      | 0.1474      | 0.4211      | 0.0000      | 0.0526      |
| 8               | 4.33                  | 0.1389      | 0.3426      | 0.0370      | 0.3611      | 0.0185      | 0.1019      |
|                 | 6.28                  | 0.1390      | 0.3632      | 0.0852      | 0.3094      | 0.0179      | 0.0852      |
|                 | 10.99                 | 0.1261      | 0.3782      | 0.1176      | 0.2857      | 0.0168      | 0.0756      |
| 9               | 4.72                  | 0.1230      | 0.4672      | 0.0328      | 0.2459      | 0.0328      | 0.0984      |
|                 | 6.70                  | 0.1174      | 0.4507      | 0.0376      | 0.2770      | 0.0376      | 0.0798      |
|                 | 8.51                  | 0.1169      | 0.4351      | 0.0325      | 0.2857      | 0.0455      | 0.0844      |
| 10              | 4.61                  | 0.0682      | 0.2614      | 0.1818      | 0.3295      | 0.0227      | 0.1364      |
|                 | 5.48                  | 0.0897      | 0.2483      | 0.1586      | 0.3241      | 0.0207      | 0.1586      |
|                 | 6.31                  | 0.0980      | 0.2255      | 0.1569      | 0.3333      | 0.0294      | 0.1471      |

The optimal regression equation in the research was obtained by using the stepwise regression method [31,32]. Stepwise regression analysis is one of the multiple regression analyses. It is often used to study the dependence among variables and establish the optimal regression model. Based on the partial regression square sum test, stepwise regression gradually introduces new variables, screens and eliminates insignificant variables and repeats until no new variables are introduced. The independent variables selected by this method have a significant effect on the dependent variables. The obtained regression equation is the required optimal model.

### 3.3.1. Definition of Velocity Collection Area

Independent riding behavior consists of deceleration riding behavior, original-speed riding behavior, acceleration riding behavior, straight riding behavior and detour riding behavior. Detour riding behavior can be divided into left detour riding behavior and right detour riding behavior. Whereas  $T_L$  represents the two-wheeler riders who choose left detour riding behavior,  $T_R$  represents the two-wheeler riders who choose right de-

tour riding behavior. The selected probability of independent riding behavior meets the following conditions:

$$P(M) = \begin{cases} P(S_1) + P(S_2) + P(S_3) = 1 \\ P(T_1) + P(T_2) = 1 \\ P(T_1) + P(T_L) + P(T_R) = 1 \end{cases} \quad (10)$$

The selected probability model of speed riding behavior that has been preliminarily fitted is shown in Table 6. The test results of the selected probability model of preliminarily fitted speed riding behavior are shown in Table 7. In Table 6  $R_A^2$  is the adjusted goodness of fit. In Table 7,  $t$  is the statistical test value. Relationship between probability of deceleration behavior, probability of original-speed behavior, probability of acceleration behavior and main influencing factors respectively are shown in Figures 11–13.

**Table 6.** Relationship between speed riding behavior probability and influencing factors.

| Riding Behavior | Regression Model                        | $R_A^2$ |
|-----------------|---|---------|
| Deceleration    | $P_0(S_1) = 0.118D + 1.046C_p - 0.744$  | 0.941   |
| Original-speed  | $P_0(S_2) = -0.115D + 1.162C_p - 0.213$ | 0.900   |
| Acceleration    | a                                       | 0.821   |

**Table 7.** Test results of probability model of speed riding behavior.

| Model  | Variable      | Coefficient | Standard Error | $t$     | Significance |
|--|---------------|-------------|----------------|---------|--------------|
| Probability model of deceleration behavior   | Constant term | −0.744      | 0.143          | −5.193  | 0.000        |
|  | $D$           | 0.118       | 0.006          | 20.259  | 0.000        |
|  | $C_p$         | 1.046       | 0.179          | 5.859   | 0.000        |
| Probability model of original-speed behavior | Constant term | −0.213      | 0.179          | −1.186  | 0.246        |
|  | $D$           | −0.115      | 0.007          | −15.744 | 0.000        |
|  | $C_p$         | 1.162       | 0.224          | 5.200   | 0.000        |
| Probability model of acceleration behavior   | Constant term | 1.853       | 0.163          | 11.378  | 0.000        |
|  | $C_p$         | −2.144      | 0.200          | −10.721 | 0.000        |
|  | $q_f$         | 0.005       | 0.002          | 3.240   | 0.003        |

The selected probability of deceleration riding behavior has a linear relationship with the subsidence depth of the manhole cover and the lane integrity. Both are positively correlated. The selected probability of original-speed riding behavior has a linear relationship with the subsidence depth of the manhole cover and the lane integrity. It is negatively correlated with the subsidence depth of the manhole cover and is positively correlated with the lane integrity. The selected probability of acceleration riding behavior is negatively linearly correlated with the lane integrity and is positively linearly correlated with the section flow.

$P'_0(S_i)$ , ( $i = 1, 2, 3$ ) are the selected probability results of each speed riding behavior initially calculated by the preliminary fitted model of  $P_0(S_i)$ , ( $i = 1, 2, 3$ ). When  $P'_0(S_i) < 0$ ,  $P'_0(S_i) > 1$  or  $\sum P'_0(S_i) \neq 1$ , to conform to the probability characteristics, the selected probability results of each speed riding behavior initially calculated by the preliminary fitted model need to be modified.  $P(S_i)$ , ( $i = 1, 2, 3$ ) are the modified selected probability results of each speed riding behavior. Since the probability value cannot be less than 0, according to the amendment rules, if  $P'_0(S_i) \leq 0$ ,  $P'_0(S_i) = 0$ . The modified selected probability model of each speed riding behavior is shown in Equation (11).

$$\begin{cases} P(S_i) = \frac{P_0(S_i)}{\sum P_0(S_i)}, i = 1, 2, 3 \\ 0 \leq P_0(S_i) \leq 1, i = 1, 2, 3 \\ \sum P_0(S_i) = 1, i = 1, 2, 3 \end{cases} \quad (11)$$

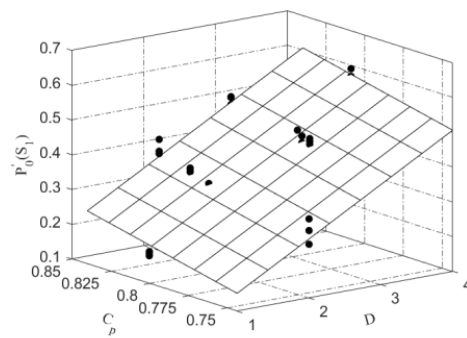


**Figure 11.** Relationship between probability of deceleration behavior and main influencing factors.

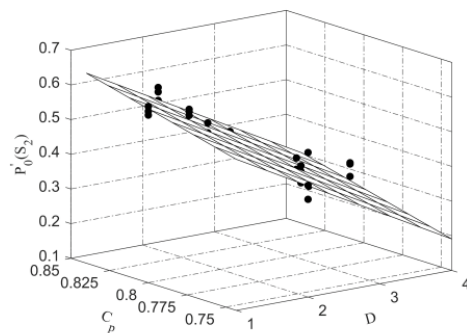


**Figure 12.** Relationship between probability of original-speed behavior and main influencing factors.

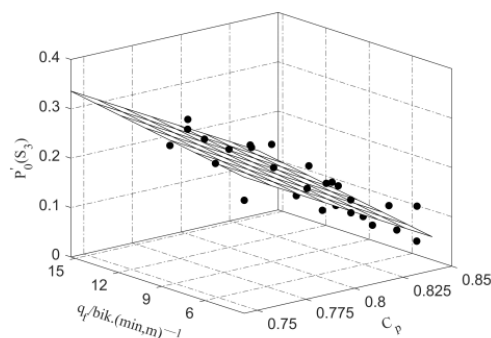


**Figure 13.** Relationship between probability of acceleration behavior and main influencing factors.

The major width of flat part and the minor width of flat part on the left or right side will affect the selected probabilities of left detour riding behavior and right detour riding behavior. The value of major width of flat part and the value of minor width of flat part are processed when constructing the selected probability model of left detour riding behavior and right detour riding behavior. In this study, the positive and negative value are used to identify the left and right position, respectively. Positive value represents that the width of the flat part is on the right side of subsidence area along the riding direction. Negative value represents that the width of the flat part is on the left side of subsidence area along the riding direction.  $C_{m1}$  is defined as the processed major width of flat part.  $C_{m2}$  is defined as the processed minor width of flat part. The selected probability model of trajectory riding behavior preliminarily fitted is shown in Table 8. The test results of selected probability model of trajectory riding behavior preliminarily fitted are shown in Table 9. Relationships between probability of straight riding behavior, probability of detour riding behavior and main influencing factors are respectively shown in Figures 14 and 15.

**Table 8.** Relationship between probability of trajectory riding behavior and influencing factors.

| Riding Behavior              | Regression Model   | $R_A^2$ |
|------------------------------|--|---------|
| Straight riding behavior     | $P_0(T_1) = -0.049D - 0.149C_{min} + 0.542$                      | 0.601   |
| Detour riding behavior       | $P_0(T_2) = 0.049D + 0.151C_{min} + 0.456$                       | 0.603   |
| Left detour riding behavior  | $P_0(T_L) = 0.185D + 0.099C_{m2} - 0.278p_2 + 0.404$             | 0.833   |
| Right detour riding behavior | $P_0(T_R) = -0.105D + 1.008C_p - 0.103C_{m2} + 0.232p_2 - 0.610$ | 0.807   |

**Table 9.** Test results of probability model of trajectory riding behavior.

| Model   | Variable      | Coefficient | Standard Error | t       | Significance |
|---|---------------|-------------|----------------|---------|--------------|
| Probability model of straight riding behavior     | Constant term | 0.542       | 0.045          | 12.029  | 0.000        |
|   | D             | -0.049      | 0.013          | -3.807  | 0.001        |
|   | $C_{min}$     | -0.149      | 0.048          | -3.119  | 0.004        |
| Probability model of detour riding behavior       | Constant term | 0.456       | 0.045          | 10.140  | 0.000        |
|   | D             | 0.049       | 0.013          | 3.786   | 0.001        |
|   | $C_{min}$     | 0.151       | 0.048          | 3.177   | 0.004        |
| Probability model of left detour riding behavior  | Constant term | 0.401       | 0.061          | 6.535   | 0.000        |
|   | D             | 0.185       | 0.026          | 7.229   | 0.000        |
|   | $C_{m2}$      | 0.099       | 0.011          | 9.142   | 0.000        |
|   | $p_2$         | -0.278      | 0.068          | -4.058  | 0.000        |
| Probability model of right detour riding behavior | Constant term | -0.610      | 0.311          | -1.962  | 0.061        |
|   | D             | -0.105      | 0.023          | -4.494  | 0.000        |
|   | $C_p$         | 1.008       | 0.387          | 2.607   | 0.015        |
|   | $C_{m2}$      | -0.103      | 0.010          | -10.381 | 0.000        |
|   | $p_2$         | 0.232       | 0.062          | 3.710   | 0.001        |

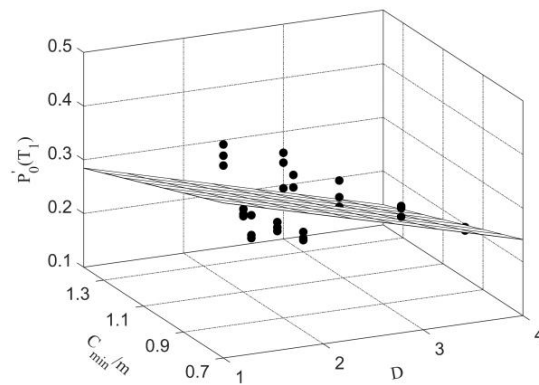


**Figure 14.** Relationship between probability of straight riding behavior and main influencing factors.

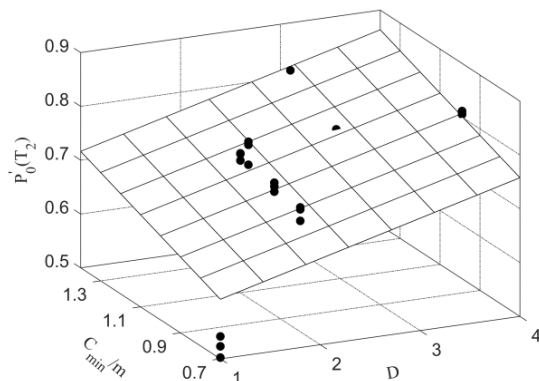


**Figure 15.** Relationship between probability of detour riding behavior and main influencing factors.

The selected probability of straight riding behavior and the selected probability of detour riding behavior have a linear relationship with the subsidence depth of the manhole cover and the minor width of the flat part. The selected probability of straight riding behavior has a negative correlation with the subsidence depth of the manhole cover and the minor width of the flat part. The selected probability of detour riding behavior is positively correlated with the subsidence depth of the manhole cover and the minor width of the flat part. The selected probability of left detour riding behavior is linear with the subsidence depth of the manhole cover, processed minor width of the flat part and the gender composition ratio of riders. The selected probability of left detour riding behavior is positively correlated with the subsidence depth of the manhole cover and processed minor width of the flat part. It is negatively correlated with the gender composition ratio of riders. The selected probability of right detour riding behavior has a linear relationship with the subsidence depth of the manhole cover, lane integrity, processed minor width of flat part and rider gender composition ratio. It is positively correlated with lane integrity and the gender composition ratio of riders, and negatively correlated with the processed minor width of the flat part.

$T_2 = T_L \cup T_R$  is known and  $P'_0(T_j)$ , ( $j = 1, 2$ ) and  $P'_0(T_k)$ , ( $j = L, R$ ) are the selected probability results of each trajectory riding behavior calculated by the preliminarily fitted model  $P_0(T_j)$ , ( $j = 1, 2$ ) and  $P_0(T_k)$ , ( $j = L, R$ ). When  $P'_0(T_j) < 0$ ,  $P'_0(T_j) > 1$ ,  $P'_0(T_k) < 0$ ,  $P'_0(T_k) > 1$ ,  $\sum P'_0(T_j) \neq 1$  or  $\sum P'_0(T_k) \neq P'_0(T_2)$ , to conform to the probability characteristics, the selected probability results of each trajectory riding behavior initially calculated by the preliminary fitted model need to be modified.  $P(T_j)$ , ( $j = 1, 2$ ) and  $P(T_k)$ , ( $j = L, R$ ) are the modified selected probability results of each trajectory riding behavior. Since the probability value cannot be less than 0, according to the amendment rules, if  $P'_0(T_j) \leq 0$ ,  $P_0(T_j) = 0$ ; if  $P'_0(T_k) \leq 0$ ,  $P_0(T_k) = 0$ . The modified selected probability model of each trajectory riding behavior is shown in Equation (12).

$$\begin{cases} P(T_j) = \frac{P_0(T_j)}{\sum P_0(T_j)}, j = 1, 2, 3 \\ P(T_k) = \frac{P_0(T_k)}{\sum P_0(T_k)}, k = L, R \\ 0 \leq P(T_j) \leq 1, j = 1, 2, 3 \\ 0 \leq P(T_k) \leq 1, k = L, R \\ \sum P(T_j) = 1, j = 1, 2, 3 \\ P(T_1) + \sum P(T_k) = 1, k = L, R \end{cases} \quad (12)$$

### 3.3.2. Selected Probability Model of Combined Riding Behavior

Combined riding behavior consists of deceleration straight riding behavior, deceleration detour riding behavior, original-speed straight riding behavior, original-speed detour riding behavior, acceleration straight riding behavior, and acceleration detour riding behavior. The probability of combined riding behavior meets the following conditions in Equation (13):

$$P(S_1T_1) + P(S_1T_2) + P(S_2T_1) + P(S_2T_2) + P(S_3T_1) + P(S_3T_2) = 1 \quad (13)$$

The selected probability model of combined riding behavior, preliminarily fitted, is shown in Table 10. The test results of the probability model of the preliminarily fitted combined riding behavior are shown in Table 11. Relationship between probability of deceleration detour riding behavior, probability of original-speed straight riding behavior, probability of acceleration straight riding behavior, probability of acceleration detour riding behavior and main factors are respectively shown in Figures 16–19.

**Table 10.** Relationship between probability of combined riding behavior and influencing factors.

| Riding Behavior                         | Regression Model  | $R_A^2$ |
|---|---|---------|
| Deceleration straight riding behavior   | $P_0(S_1 T_1) = 0.021D - 0.017C_{max} + 0.030p_1 + 0.063$ | 0.603   |
| Deceleration detour riding behavior     | $P_0(S_1 T_2) = 0.096D + 1.160C_p - 0.892$                | 0.877   |
| Original-speed straight riding behavior | $P_0(S_2 T_1) = -0.063D - 0.081C_{min} + 0.354$           | 0.795   |
| Original-speed detour riding behavior   | $P_0(S_2 T_2) = -0.033D + 0.682C_p - 0.006q_f - 0.097$    | 0.503   |
| Acceleration straight riding behavior   | $P_0(S_3 T_1) = -0.025C_{max} - 0.117C_{min} + 0.215$     | 0.595   |
| Acceleration detour riding behavior     | $P_0(S_3 T_2) = -1.564C_p + 0.006q_f + 1.343$             | 0.715   |

**Table 11.** Test results of probability model of combination riding behavior.

| Model  | Variable      | Coefficient | Standard Error | t      | Significance |
|--|---------------|-------------|----------------|--------|--------------|
| Probability model of deceleration straight riding behavior   | Constant term | 0.063       | 0.025          | 2.522  | 0.020        |
|  | D             | 0.021       | 0.005          | 4.524  | 0.000        |
|  | $C_{max}$     | -0.017      | 0.006          | -2.723 | 0.013        |
|  | $p_1$         | 0.030       | 0.013          | 2.291  | 0.033        |
| Probability model of deceleration detour riding behavior     | Constant term | -0.892      | 0.181          | -4.935 | 0.000        |
|  | D             | 0.096       | 0.007          | 13.043 | 0.000        |
|  | $C_p$         | 1.160       | 0.225          | 5.147  | 0.000        |
| Probability model of original-speed straight riding behavior | Constant term | 0.354       | 0.028          | 12.602 | 0.000        |
|  | D             | -0.063      | 0.008          | -7.820 | 0.000        |
|  | $C_{min}$     | -0.081      | 0.030          | -2.734 | 0.011        |
| Probability model of original-speed detour riding behavior   | Constant term | -0.097      | 0.226          | -0.430 | 0.670        |
|  | D             | -0.033      | 0.010          | -3.498 | 0.002        |
|  | $C_p$         | 0.682       | 0.279          | 2.445  | 0.022        |
|  | $q_f$         | -0.006      | 0.002          | -2.418 | 0.023        |
| Probability model of acceleration straight riding behavior   | Constant term | 0.215       | 0.027          | 7.995  | 0.000        |
|  | $C_{max}$     | -0.025      | 0.007          | -3.787 | 0.001        |
|  | $C_{min}$     | -0.117      | 0.019          | -6.280 | 0.000        |
| Probability model of acceleration detour riding behavior     | Constant term | 1.343       | 0.169          | 7.942  | 0.000        |
|  | $C_p$         | -1.564      | 0.208          | -7.536 | 0.000        |
|  | $q_f$         | 0.006       | 0.002          | 3.366  | 0.002        |

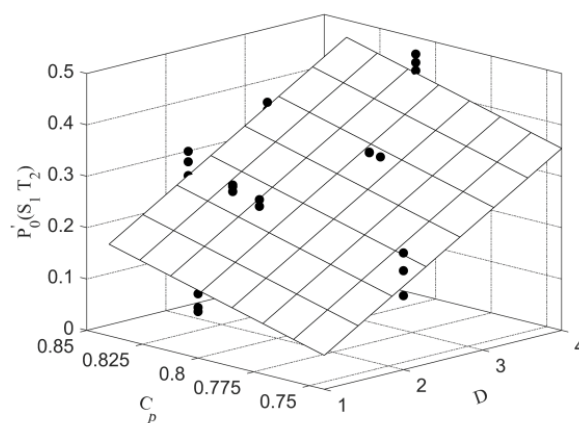


**Figure 16.** Relationship between probability of deceleration detour riding behavior and main factors.

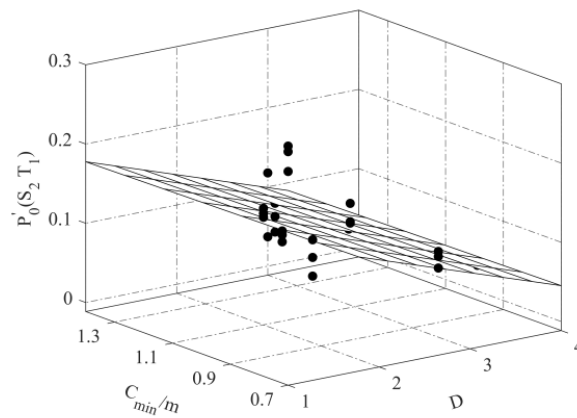


**Figure 17.** Relationship between probability of original-speed straight riding behavior and main factors.

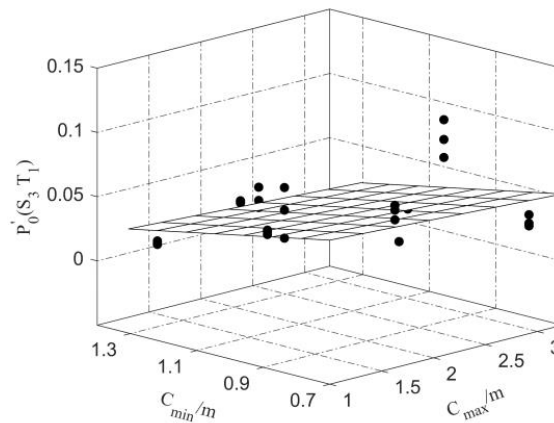


**Figure 18.** Relationship between probability of acceleration straight riding behavior and main factors.

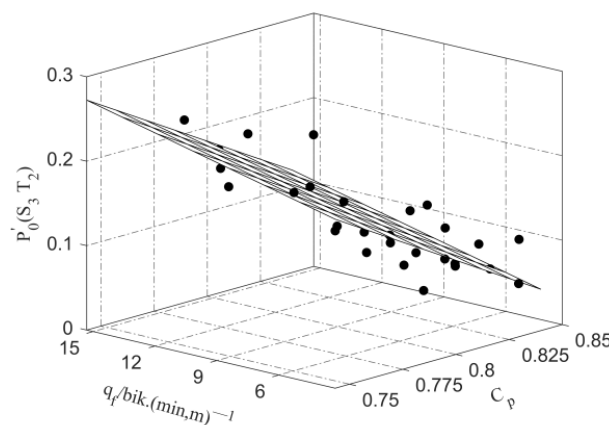


**Figure 19.** Relationship between probability of acceleration detour riding behavior and main factors.

The selected probability of deceleration straight riding behavior has a linear relationship with the subsidence depth of the manhole cover, major width of the flat part and the age composition ratio of riders. It is positively correlated with the subsidence depth of the manhole cover and the age composition ratio of riders. It is negatively correlated with the major width of the flat part. The selected probability of deceleration detour riding behavior has a linear relationship with the subsidence depth of the manhole cover and lane integrity. They are positively correlated. The selected probability of original-speed straight riding behavior has a linear relationship with the subsidence depth of the manhole cover and the minor width of the flat part. Both have a negative correlation. The selected probability of

original-speed detour riding behavior has a linear relationship with the subsidence depth of the manhole cover, lane integrity and section flow. It is positively correlated with lane integrity and negatively correlated with the subsidence depth of the manhole cover and section flow. The selected probability of acceleration straight riding behavior has a linear relationship with the major width of the flat part and the minor width of the flat part. Both have a negative correlation. The selected probability of acceleration detour riding behavior has a linear relationship with the lane integrity and the section flow. It has a positive correlation with the section flow. It is negatively correlated with the lane integrity.

$P'_0(S_iT_j)$ , ( $i = 1, 2, 3, j = 1, 2$ ) are the selected probability models of each combined riding behavior calculated by the preliminary fitted model  $P_0(S_iT_j)$ , ( $i = 1, 2, 3, j = 1, 2$ ). When  $P'_0(S_iT_j) < 0$ ,  $P'_0(S_iT_j) > 1$  or  $\sum P'_0(S_iT_j) \neq 1$ , to conform to the probability characteristics, the selected probability results of each combined riding behavior initially calculated by the preliminary fitted model need to be modified.  $P(S_iT_j)$ , ( $i = 1, 2, 3; j = 1, 2$ ) are the selected probability results of each combined riding behavior. Since the probability value cannot be less than 0, if  $P'_0(S_iT_j) \leq 0$ ,  $P'_0(S_iT_j) = 0$ . The modified selected probability model of combined riding behavior is shown in Equation (14).

$$\begin{cases} P(S_iT_j) = \frac{P_0(S_iT_j)}{\sum P_0(S_iT_j)}, i = 1, 2, 3, j = 1, 2 \\ 0 \leq P(S_iT_j) \leq 1, i = 1, 2, 3, j = 1, 2 \\ \sum P(S_iT_j) = 1, i = 1, 2, 3, j = 1, 2 \end{cases} \quad (14)$$

#### 4. Discussion

This paper classifies riders' riding behaviors and analyzes the influences of seven major factors on their riding behavior choices under the subsidence of manhole cover conditions.

- (1) The results in Figures 6 and 7 show that under the subsidence of manhole cover conditions, when the speed reaches a great value ( $v \geq 10.4$  m/s) or a very small value ( $v \leq 2.7$  m/s), two-wheelers have almost no speed change and detour behavior. The reasons are as follows: when the two-wheelers reach the sight distance where the manhole cover can be recognized and identified, the faster the two-wheeler speed is, the less reaction time and operation time for the rider; when the speed reaches a great value, the rider allocates more attention to observe the surrounding disturbance (such as observing the surrounding disturbing pedestrians or disturbing vehicles) to improve the safety of riding, but ignores the observation of the road condition, which in turn leads to a situation where the rider cannot make effective behavior to avoid or improve the comfort of passing when encountering the manhole cover; when the traffic density is very high or the investigated two-wheeler is a human-powered bicycle, the speed may reach a very small value, the impact of the manhole cover on the two-wheeler is minimal and the two-wheeler can pass through the subsidence area without changing its riding behavior.
- (2) The results show that the subsidence depth was positively correlated with the probability of deceleration behavior and negatively correlated with original-speed behavior (as shown in Figure 20); lane integrity was positively correlated with the probability of deceleration and original-speed behavior (as shown in Figure 21). The reasons are as follows: the subsidence depth is an influencing factor for the rider to get the information intuitively. The rider can quickly make the judgment of deceleration or original-speed behavior after getting the information of subsidence depth within sight distance and confirming that there is no interference in the surrounding area to improve the riding comfort and safety. In addition, lane integrity is also an important influencing factor. Since the transverse cross-sectional width of the manhole cover sinkhole area is similar, the lane integrity can indirectly reflect the bicycle lane width. If the transverse width of the manhole cover area is the same, the greater the lane integrity, the greater the bicycle lane width. Under similar flow conditions, the greater the lane width, the lower the traffic density and the greater the spacing between

two-wheelers. Under low-density conditions, there are fewer two-wheelers on the road that can interfere with riders, and the headways are larger, so riders can detect and discern the subsidence of manhole covers at a greater distance. This gives riders sufficient distance, reaction time and attention to make judgments about deceleration or original-speed behavior.

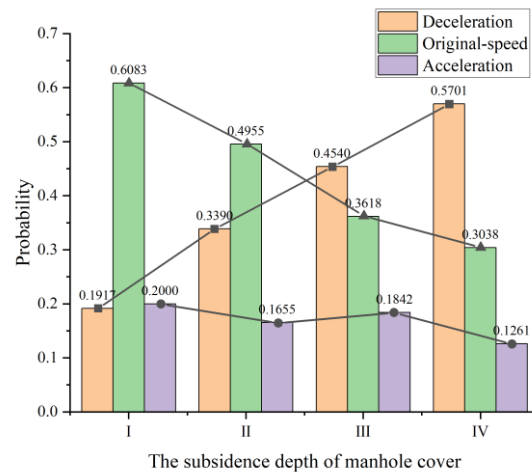


**Figure 20.** Relationship between subsidence depth of the manhole cover and selected probability of speed riding behavior.

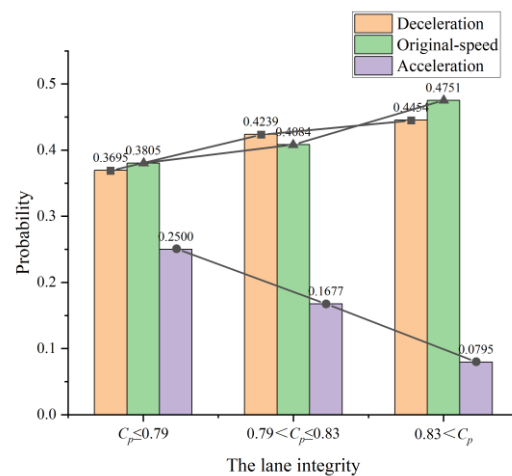


**Figure 21.** Relationship between lane integrity and selected probability of speed riding behavior.

- (3) Under the subsidence of manhole cover conditions, acceleration riding behavior is more specific riding behavior. The results show that the probability of this behavior is less correlated with the subsidence depth of the manhole cover, but negatively correlated with lane integrity (as shown in Figure 21) and positively correlated with section flow (as shown in Figure 22). The reasons are as follows: Acceleration behavior is essentially influenced by the driving force of social forces; Liang et al. [33] proposed that, in a specific scenario, the rider is motivated to move towards the destination according to the desired speed at a certain speed, and the force driving the behavior is called the driving force, which is a psychological force. When riders choose to go around to avoid the subsidence to obtain better riding comfort, if there are interfering vehicles behind, this behavior will increase the mutual interference between vehicles, and riders wishing to move laterally safely and comfortably need to improve their longitudinal spacing from interfering vehicles to the side and rear, increasing the rider's detour safe operating distance and operable time, and the rider's desired speed is greater than the actual operating speed, thus choosing acceleration riding

behavior. Two-wheelers, to avoid the subsidence area, pass from both sides of the manhole cover when the lane width is certain, and the smaller the lane integrity, the smaller the complete lane width on both sides of the manhole cover and the greater the mutual interference between the two-wheelers from the side and rear when detouring; similarly, the higher the section flow, the more interfering two-wheelers there are around the investigated two-wheeler, and the more interference from the side and rear two-wheelers when the two-wheeler detours. Influenced by the driving force, the greater the disturbance, the higher the probability of riders choosing acceleration riding behavior, and the same analytical conclusion can be drawn from the acceleration detour riding behavior selection model in this paper. In summary, acceleration is a riding behavior resulting from the conflict between the rider's desire to reduce interference with surrounding two-wheelers and his desire for a more comfortable riding experience.

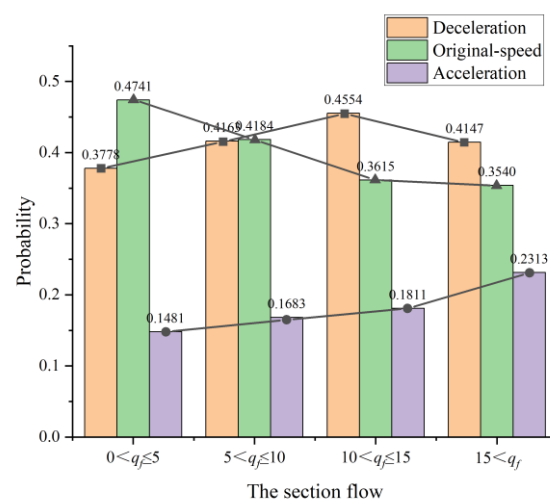


**Figure 22.** Relationship between section flow and selected probability of speed riding behavior.

- (4) The research findings for trajectory riding behavior show that the subsidence depth of manhole covers is negatively correlated with straight riding behavior and positively correlated with detour riding behavior (as shown in Figure 23); the minor width of the flat part is negatively correlated with straight riding behavior and positively correlated with detour riding behavior (as shown in Figure 24). The reasons are analyzed as follows: as mentioned in discussion (2), the information about the subsidence depth of the manhole cover can be intuitively received by the rider, and the judgment of whether to crush the subsidence or not can be made quickly after observing the surrounding conditions. The minor width of the flat part describes how far the manhole cover is from the hard separation boundary of the lane; the smaller the value, the closer the manhole cover is to the boundary. When a rider wishes to avoid a manhole cover, he or she will choose to pass in the direction that is fastest away from the upstream virtual traffic zone, which is the direction where the two-wheeler is close to the edge line of the upstream virtual traffic zone. Liang et al. [33] in the existing research proposed a lane boundary force, which is a psychological force; hard separation facilities will bring a feeling of discomfort and insecurity to riders, the closer the vehicle is to the road hard separation boundary, the more the vehicle will try to run away from the boundary; therefore, when the manhole cover is close to the lane boundary, the vehicle running close to the lane boundary side in the upstream virtual traffic zone, which is affected by the boundary force, does not choose to pass by the flat part on the boundary side, but chooses not to change direction to run over the manhole cover to pass. From the probability model of original-speed straight riding behavior, it is clear that the minor width of the flat part is negatively correlated with the probability of original-speed detour riding behavior. Liang et al. [34] found that,

the closer the bicycle lane area is to the lane boundary, the higher the percentage of low-speed vehicles and the lower the percentage of high-speed vehicles, and since the subsidence of the manhole cover has less impact on low-speed vehicles, more riders riding at low speeds near the lane boundary side tend to adopt the original-speed straight riding behavior to pass through the subsidence area.

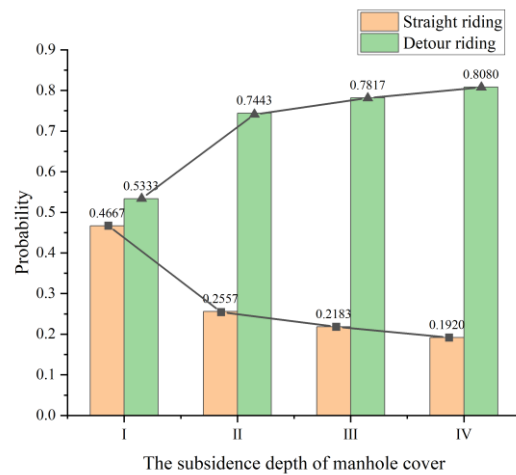


**Figure 23.** Relationship between subsidence depth of the manhole cover and selected probability of trajectory riding behavior.

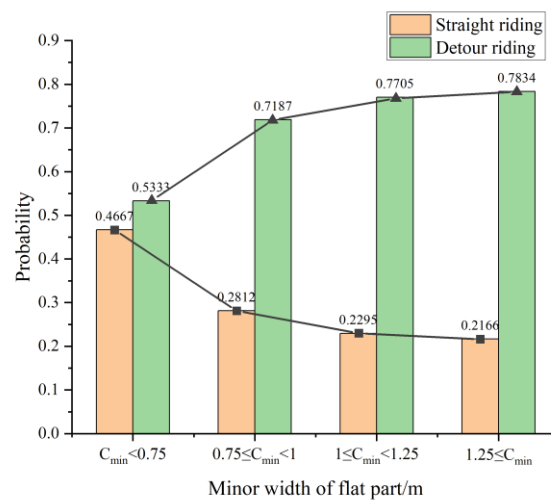


**Figure 24.** Relationship between minor width of the flat part and selected probability of trajectory riding behavior.

- (5) In addition to the correlation with the subsidence depth of the manhole cover, the probability of deceleration straight riding behavior also has a strong correlation with the major width of the flat part, which is negatively correlated with the major width of the flat part. The reasons are as follows: the major width of flat part can describe how far the manhole cover is from the bicycle lane centerline; when the major width of flat part is smaller, the closer the manhole cover is to the lane median. (1) It is known from the literature [34] that the closer the riding area is to the lane centerline, the higher the proportion of medium- and high-speed vehicles that pass within it; from discussion (1), it is clear that the faster the speed of the two-wheeler, the less reaction time and operation time the rider has; from the literature [35], it is clear that when the speed is high, the two-wheeler cannot change the turning angle at a large angle for safety. Therefore, when the rider passes at a faster speed, he finds and discriminates the subsidence area and judges that the speed and distance cannot meet the requirement

of avoiding the subsidence area at this time, so the rider chooses deceleration riding behavior to improve comfort when running over the subsidence area. (1) The closer the subsidence of the manhole cover is to the centerline of the bicycle lane, the greater the interference of traffic on both sides of the upstream virtual traffic zone. When the rider's fastest out of the upstream virtual traffic zone direction side of a more serious interference, subject to the collision avoidance forces proposed in the literature [33], the rider will be forced to choose deceleration straight riding behavior through the subsidence area with high probability.

There are some shortcomings in this research. Constrained by the difficulty of data acquisition, this paper mainly considers the subsidence of the manhole cover and road environment-related factors and does not consider the influence of disturbance factors outside the bicycle lane on riding behavior. During the investigation, the investigators found that some external factors also have an impact on riding behavior, such as ambient light conditions, shade and surrounding environmental sounds, but the data for these related factors are difficult to collect and quantify. It is hoped that solutions can be found in future studies.

Follow-up research work can continue to explore the psychological and physiological effects of manhole cover subsidence on two-wheeler riders by using oculomotor and physiological recorders and conducting surveys in two-wheeler simulators or in the field to obtain the physiological and psychological changes of riders when experiencing the subsidence of the manhole cover.

## 5. Conclusions

This paper uses multiple regression analysis to investigate the influence of each major influencing factor on the selected probability of riding behavior. The results are as follows:

- (1) Bicycle road sections with low traffic volumes and a lack of traffic control on the periphery of the city have a higher probability of very high-speed two-wheelers. If the road surface of these sections is not maintained for a long time, creating a more serious problem of manhole cover subsidence, it is very likely to cause traffic safety problems. In contrast, the subsidence of manhole covers has less impact on two-wheelers operating in high-density environments.
- (2) Subsidence depth is one of the main factors affecting riders' riding behavior, and it has a great influence on the selection of riders' speed and trajectory behavior; the influence of subsidence of grade I and below on riders is small; the influence of grade II and above on riders is large, especially the depression of grade IV, which is likely to cause safety problems.
- (3) The narrower the bicycle lane and the higher the traffic flow, the greater the probability that the rider will choose the acceleration detour riding behavior, the greater the impact of subsidence of the manhole cover on traffic flow. The acceleration detour riding behavior is a riding behavior resulting from the conflict between the rider's desire to reduce mutual interference with surrounding two-wheelers and his desire for a more comfortable riding experience. This paper shows that it is important for riders to obtain information about the movement of the two-wheelers behind them when operating the lateral movement.
- (4) The closer the manhole cover is to the lane boundary, the less it affects two-wheelers and the less it interferes with traffic flow. The closer the manhole cover is to the lane centerline, however, the greater the impact on two-wheelers and the greater the disruption to traffic flow operations.

## 6. Applications and Suggestions

- (1) City managers and traffic managers should pay more attention to bicycle roads with low traffic volume and a lack of traffic control on the periphery of the city and regularly inspect the pavement conditions of these roads. If there is a subsidence of grade IV, it should be repaired and maintained in time. If maintenance cannot be carried out

in time, it is recommended to set up a prompt sign at the exit road of the upstream intersection of the road section to indicate that there is a serious pavement damage problem ahead and ask two-wheelers to slow down, and the same prompt sign should be set up 30 m upstream of the subsidence.

- (2) Subsidence of level I does not need much repair treatment. Selective repair treatment is determined by the position of the level II or III in the section, section flow and lane width. Subsidence of level IV should be repaired as soon as possible.
- (3) Although the subsidence of manhole covers in major bicycle lanes in cities with narrower lanes and higher traffic flow is unlikely to cause safety issues, it will affect the riding comfort of a large number of riders and is likely to disrupt traffic flow operation due to higher traffic flow and density. Subsidence of manhole covers in main bicycle lanes in cities with small lanes should be addressed as soon as possible, and if this is not possible, reflective strips can be plastered on the manhole covers to improve visibility of the subsidence of manhole covers.
- (4) When comparing the subsidence of manhole covers near the lane boundary to the subsidence of manhole covers near the lane centerline, city managers should pay more attention to the subsidence of manhole covers near the lane centerline, which has a greater impact on the operation of two-wheelers; if such covers have more serious subsidence problems, they should be dealt with quickly.
- (5) Traffic managers should strengthen the education of riders by considering the following: (1) They should educate riders to develop the habit of looking in the rearview mirror when the two-wheeler is in lateral motion. Riders must examine the rear two-wheeler activity through the rearview mirror because the low noise of the two-wheeler operation makes it impossible for them to notice the rear hazard more thoroughly through hearing alone. (2) They should educate riders on how to adjust the best angle of the rearview mirror according to their height, sitting posture and riding habits. (3) They should educate riders to prohibit wearing headphones or any clothing or accessories that cover or wrap the ears during riding. This behavior can enhance the ability of riders to perceive the surrounding hazards through hearing.
- (6) Traffic managers should strengthen the inspection of two-wheelers and strictly check two-wheelers without rearview mirrors, and shared bicycle companies should also install rearview mirrors on the shared two-wheelers they put out.

**Author Contributions:** Conceptualization, D.Z. and Q.H.; methodology, D.Z. and Q.H.; software, Q.H. and C.M.; validation, D.Z., Q.H. and G.G.; formal analysis, D.Z. and Q.H.; investigation, C.M., W.Y. and G.G.; resources, Q.H. and C.M.; data curation, D.Z., Q.H. and G.G.; writing—original draft preparation, D.Z., Q.H. and X.S.; writing—review and editing, D.Z., Q.H. and X.S.; visualization, D.Z., Q.H. and R.Y.; supervision, D.Z., Q.H. and W.Y.; project administration, Q.H.; and funding acquisition, D.Z. All authors have read and agreed to the published version of the manuscript.

**Funding:** This work was supported by the National Natural Science Foundation of China (grant no. 71861005).

**Institutional Review Board Statement:** Not applicable.

**Informed Consent Statement:** Not applicable.

**Data Availability Statement:** The data used in the study are available from the corresponding author upon request.

**Conflicts of Interest:** The authors declare that they have no conflict of interest.

## References

- Xiong, W.H.; Wei, D. Impaction Analysis of Motorcycle Forbidden Policy's upon Resident's Traveling Time Cost. *J. Transp. Syst. Eng. Inf. Technol.* **2013**, *13*, 203–208. [CrossRef]
- Zhao, D.; Li, S.J. Economic analysis of urban motorcycle bans—Nanning City as an example. *Leg. Econ.* **2016**, 57–58. Available online: <https://kns.cnki.net/kcms/detail/detail.aspx?dbcode=CJFD&dbname=CJFDLAST2016&filename=FZJJ201607017&uniplatform=NZKPT&v=gtaj7qgUXNurp7ixgIhOutwmAQK6p2JVJ7wdivDTuAz7DPYnTd2gX8NxU11BSSfK> (accessed on 14 July 2016).
- Nie, X. A study on the current development of urban non-motorized transportation in China. *New Technol. New Prod. China* **2016**, *21*, 126. [CrossRef]
- Kuang, L.J.; Ye, X.F. Characteristics of Bike-and-Ride at Urban Mass Transit Station. *Urban Mass Transit* **2010**, *13*, 53–56. [CrossRef]
- Zhao, Q.M.; Ren, R.B.; Liu, Y.; Li, Z.G.; Hu, G.L. Fracture Mechanism of Pavement around Manholes in Urban Road. *J. Chongqing Jiaotong Univ. (Nat. Sci.)* **2021**, *40*, 87–94.
- Yv, T.G.; Jiang, C.J.; Cao, X.Y. Quality Defects Treatment of Municipal Roads Inspection Wells. *Constr. Technol.* **2014**, *43*, 291–293.
- Mastinu, G.; Ploechl, M. *Road and Off-Road Vehicle Systemdynamics Handbook*; CRC Press: Boca Rato, FL, USA, 2014; pp. 21–25.
- Wang, X.R.; Zhang, J.X.; Kong, X.G. Asphalt Pavement Damage Evaluation Based on Riding Comfort. *Munic. Eng. Technol.* **2014**, *32*, 32–36.
- Shan, L.Y.; Hou, X.S. Analysis of the relationship between pavement unevenness and driving comfort based on the whole vehicle model. *Highway* **2005**, 122–125. Available online: <https://kns.cnki.net/kcms/detail/detail.aspx?dbcode=CJFD&dbname=CJFD2005&filename=GLGL200508029&uniplatform=NZKPT&v=HA55WY4YtFY6INiG6QRKpOknwco8a86CUBVixBgpXxq0jZcaTuofZGpQ-HV81V1> (accessed on 25 August 2005).
- Shan, L.Y.; Hou, X.S.; Ma, S.L. Evaluation standard of pavement roughness based on ride comfort. *J. Harbin Inst. Technol.* **2008**, 935–938.
- Lu, C.G.; Zhao, Q.H.; Zhang, H.X.; Yang, J.Z. Research on the Influence of Road Roughness, Speed and Seat Occupancy Rate on Driving Comfort Based on Simulink. *J. Qingdao Univ. (Eng. Technol. Ed.)* **2020**, *35*, 29–36. [CrossRef]
- Guan, L.M.; Wang, G.P.; Zhu, J.Y.; Wu, D.F. Prediction of driving comfort on urban road based on discrete roughness index. *J. Vib. Shock* **2021**, *40*, 236–242. [CrossRef]
- Zhao, Q.; Yuan, Q.Q. The Construction Standard of Bicycle Friendly City from the Kano Demand Model. *Mod. Transp. Technol.* **2019**, *16*, 81–87.
- Xiao, H.Z.; Qiu, X.F.; Li, L.Z.; Chen, Z.P. Evaluation Method of Comfort of Public Bicycle Routes in Xiamen. *Technol. Innov. Appl.* **2019**, 104–105.
- Cheng, G.Z.; Liu, B.T.; Ma, Y.F. Effect of Poor Pavement Surface Condition on Capacity of Urban Roadway. *Urban Transp. China* **2012**, *10*, 68–74. [CrossRef]
- Chen, H.; Ma, X.T.; Zhao, D.T. Simulation of Vehicle Lane-changing Behavior on Damaged Pavement Based on CA Model. *J. Highw. Transp. Res. Dev.* **2018**, *35*, 117–125.
- Khan, S.; Raksuntorn, W. Characteristics of Passing and Meeting Maneuvers on Exclusive Bicycle Paths. *Transportation Research Record. J. Transp. Res. Board* **2001**, *1776*, 220–228. [CrossRef]
- Chen, X.; Yue, L.; Han, H. Overtaking Disturbance on a Moped-Bicycle-Shared Bicycle Path and Corresponding New Bicycle Path Design Principles. *J. Transp. Eng.* **2018**, *144*, 4018041–4018048. [CrossRef]
- Xu, L.; Liu, M.Q.; Song, X.; Jin, S. Analytical Model of Passing Events for One-Way Heterogeneous Bicycle Traffic Flows. *Transp. Res. Rec.* **2018**, *2672*, 125–135. [CrossRef]
- Li, Z.; Wang, W.; Liu, P.; Bigham, J.; Ragland, D.R. Modelling Bicycle Passing Maneuvers on Multilane Separated Bicycle Paths. *J. Transp. Eng.* **2013**, *139*, 57–64. [CrossRef]
- Dong, P.; Wang, X.; Yun, L.; Fan, H. Research on the characteristics of mixed traffic flow based on an improved bicycle model. *Simulation* **2017**, *94*, 451–462. [CrossRef]
- Kuang, X.Y.; Cao, W.H.; Wu, Y. Cellular Automata Model of Non-motor Vehicle Flow Considering Reverse Vehicles. *J. Syst. Simul.* **2016**, *28*, 268–274. [CrossRef]
- Ping, P.; Chang, Y.L.; Zhang, P. Impact of inbound and Outbound Passengers form Bus Stop on Neighboring Bicycle Lane Capacity. *J. Chongqing Univ. Technol. (Nat. Sci.)* **2018**, *32*, 103–110.
- Wen, X.M.; Fu, L.P.; Zhao, M.; Pan, X.F. Analysis of Driving Behaviors and Pedestrian Crossing Safety on Urban Roadway with Mixed Traffic Flow. *J. Transp. Inf. Saf.* **2020**, *38*, 12–19.
- Ye, X.F.; Deng, S.J.; Chen, J.; Zhen, J.H. Impact of Curbside Parking on Bicycle Lane Capacity. *J. Southwest Jiaotong Univ.* **2015**, *50*, 529–535.
- Ye, X.F.; Chen, J.; Feng, S.M.; Deng, S.J. Model of non-motorized vehicle flow speed influenced by curbside parking. *J. Harbin Inst. Technol.* **2016**, *48*, 115–119.
- Zhang, G.Q.; Wang, H.; Chen, J. Psychological research in traffic engineering. *J. Southeast Univ. (Philos. Soc. Sci.)* **2012**, *14*, 156–159. [CrossRef]
- Editorial Department of China Journal of Highway and Transport. Review on China's Traffic Engineering Research Progress: 2016. *China J. Highw. Transp.* **2016**, *29*, 1–161. [CrossRef]

29. Zhou, D.; Ma, H.L.; Jin, S.; Wang, D.H. Flow-density relationship of mixed bicycles based on Logistic model. *J. Traffic Transp. Eng.* **2016**, *16*, 133–141. [[CrossRef](#)]
30. Wang, Y.M.; Elhag, T. On the normalization of interval and fuzzy weights. *Fuzzy Sets Syst.* **2006**, *157*, 2456–2471. [[CrossRef](#)]
31. Agostinelli, C. Robust Stepwise Regression. *J. Appl. Stat.* **2002**, *29*, 825–840. [[CrossRef](#)]
32. Burkholder, T.J.; Lieber, R.L. Stepwise Regression is An Alternative to Splines For Fitting Noisy Data. *J. Biomech.* **1996**, *29*, 235–238. [[CrossRef](#)]
33. Liang, X.; Mao, B.H.; Xu, Q. Psychological- physical force model for bicycle dynamics. *J. Transp. Syst. Eng. Inf. Technol.* **2012**, *12*, 91–97. [[CrossRef](#)]
34. Liang, X.; Xiao, Z.S.; Yuan, Y.; Huang, X. Setting Conditions and Key Parameters for Two-way Separated Bicycle Lane Design. *J. Transp. Syst. Eng. Inf. Technol.* **2016**, *16*, 227–232. [[CrossRef](#)]
35. Xv, Y.W. Talking about the running of bicycle. *J. Sichuan Vocat. Tech. Coll.* **2002**, 56–57. [[CrossRef](#)]